Energy Proceedings
Vol 50, 2025
ISSN 2004-2965

Modeling and Analysis of the Hydrogen Circulation Structure of PEMFC System#

Tiancai Ma[1,2*], Beiming Huang[1], Chongjiu Li[1], Ziheng Gu[1]

1 School of Automotive Studies, Tongji University, Shanghai, 201804, P. R. China

2 Institute of Carbon Neutrality, Tongji University, Shanghai, 200092, P. R. China
(*Corresponding Author: matiancai@tongji.edu.cn)

ABSTRACT

Hydrogen supply system needs to provide sufficient mass flow and pressure of hydrogen to meet the requirement of fuel cell stack in PEMFC system. Ejector and hydrogen circulating pump (HRP) are commonly used to recycle unreacted hydrogen to improve energy utilization and system efficiency. However, ejector can not achieve active control and has narrow efficient working range, while HRP leads to extra parasitic power. This paper establishs an accurate hydrogen supply system model and proposes single recycle component scheme and combination of ejector and HRP scheme, discussing the working performance of different circulation structure scheme. The simulation results indicate that single ejector can not recycle enough flow rate and even counterflow occurs with fuel cell system output power less than 60kW. Single HRP controls the hydrogen recycle flow rate accurately but an average of 280.1W parasitic power is consumped. In ejector and HRP parallel scheme, matching control strategy is proposed and an average of parasitic power can be reduced 190W than single HRP scheme in whole fuel cell stack working operation. In ejector and HRP serial scheme, matching strategy controls HRP establish high pressure difference to help overcome flow resistance from ejector with maximun 0.45kPa in low current loading condition. When system output power exceeds 60kW, HRP is shut off and ejector overcomes a maximun flow resistance of 22.25kPa from HRP. An average of parasitic power is reduced 200.8W than single HRP scheme.

Keywords: PEMFC, hydrogen supply system, ejector and HRP parallel scheme, ejector and HRP serial scheme

NONMENCLATURE

Abbreviations	
PEMFC	Proton exchange membrane fuel cell
HRP	Hydrogen circulating pump
STR	hydrogen stoichiometric ratio
PV	Proportional solenoid valve
MPV	Medium pressure solenoid valve
PurgV	Purge valve
Symbols	
P	Pressure
$\dot{m}$	Mass flow rate
m	Mass
R	Gas constant
T	Temperature
V	Cavity volume
A	Cavity sectional area
ρ	Gas density
λ	Drag coefficient
u	Flow velocity
M	Molar mass
N	Number of cells
I	Stack load current
F	Faraday constant
K_v	Flow coefficient
n	Motor speed of HRP
C_p	Specific heat capacity at constant pressure
C_v	Specific heat capacity at constant volume
Subcripts	
h	Hydrogen
v	Vapor
in	Inlet
out	Outlet
pv	Proportional solenoid valve
$ejct$	Ejector
hrp	Hydrogen circulating pump
an	Anode flow channel

1. INTRODUCTION

In order to meet the challenge of environmental degradation, hydrogen energy as an ideal clean energy

This is a paper for the 16th International Conference on Applied Energy (ICAE2024), Sep. 1-5, 2024, Niigata, Japan.

has become the focus of research and development[1]. Proton exchange membrane fuel cell (PEMFC) as a hydrogen energy conversion device, having high energy density and high conversion efficiency, has been widely concerned in the field of transportation and power generation due to its low operating temperature and low noise[2]. As one of the key subsystem, hydrogen supply system needs to provide sufficient flow and pressure of hydrogen to the stack to maintain the normal operation. The design of hydrogen circulation structure directly affects the fuel efficiency, durability, performance and reliability of the whole system[3].

Research on the Scheme of Hydrogen supply system has been increasingly concerned. In the flow-through scheme, the exhaust valve is fully opened and the unreacted hydrogen is discharged directly into the atmosphere. Although this scheme can avoid flooding, the direct discharge of hydrogen will cause energy waste and security risks[4]. To solve energy dissipation, Jixin Chen[5] proposed dead-end scheme that seal the anode outlet so that the unreacted hydrogen stays in the stack self-circulation, so as to passively improve the hydrogen utilization rate. However, dead-end scheme can not purge the anode liquid water leading to stack performance reduction after a period of time[6].

In addition, there are other circulation schemes used in the design of fuel cell hydrogen supply system. Badami et al[7] used a HRP to assist in recycling the unreacted hydrogen to the anode inlet. He[8] used HRP scheme and developed a control algorithm to achieve sufficient supply of hydrogen fuel and improve hydrogen utilization. Although HRP scheme has many advantages, it brings additional parasitic power, vibration and noise[9]. Therefore, ejector scheme is also used in hydrogen supply system. The ejector can passively recycle unreacted hydrogen into the supply manifold without increasing energy consumption, but its working range is narrow and uncontrollable[10]. Wang[11] designed an ejector for an 80 kW PEMFC system and verified its validity. Hwang[12] employed a vacuum ejector hybrid scheme combining a continuous supply flow and a pulse supply flow to improve a wide range of stack power consumption. Ejector and HRP parallel scheme is also used in PEMFC system[13,14]. The parallel scheme can recycle larger flow under the same pressure rise condition, which can effectively improve the working range. Ejector and HRP serial scheme is another scheme which can work in larger pressure rise without Hydrogen counterflow[15,16]. In serial scheme, HRP helps increase the secondary inlet pressure of the ejector, thereby increasing the circulating flow rate[17].

Many reseaches focused on the Ejector scheme and HRP scheme which are widely used in low power PEMFC system. But the combination of ejector and HRP scheme is more suitable for high power PEMFC system because of its characteristics of wide working range and rapid response to changes in operation conditions. However, there are few studies on the matching and control of the conbination scheme. In particular, the application scope of serial scheme and parallel scheme is not clear. In this paper, an accurate dynamic fuel cell hydrogen supply system model for simulation analysis is established. The working characteristics of different circulation schemes are discussed. The matching control strategies which aim to reduce the parasitic power are designed. This paper is structured as follows. Section 2 proposes and verifies a fuel cell hydrogen supply system model for further research. Section 3 analyses the working characteristic of single ejector circulation structure. In section 4, matching control strategy of ejector and HRP parallel scheme and serial scheme are designed disccussing recycle performance under 130 kW fuel cell system load current step condition.

2. HYDROGEN SUPPLY SYSTEM MODEL

The hydrogen supply system consists of a medium pressure solenoid valve (MPV), a proportional solenoid valve (PV), an ejector, a supply manifold, an inlet manifold, an anode flow channel, an outlet manifold, a purge valve and HRP. In order to make the analysis more comprehensive, the structure used to model in this paper is the ejector and HRP conbination scheme, shown in Fig.1. In this paper, the hydrogen and water vapor are both considered as the ideal gas and no liquid water is generated along all of manifolds. The hydrogen from the hydrogen tank is pure without water vapor or any other impurity gas. The liquid water generated in the anode flow channel is completely filtered out by the water separator.

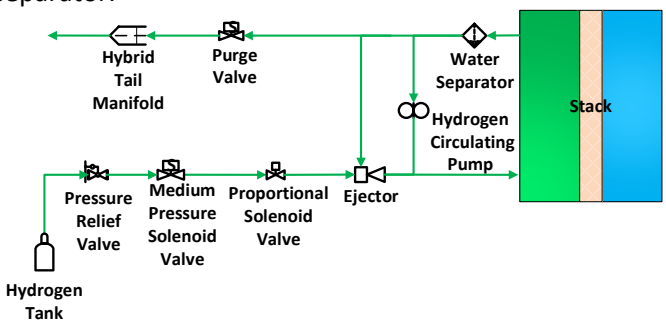

Fig.1 Hydrogen supply system structure.

2.1 Manifolds

The modeling methods of Manifolds are similar and fluid flow characteristic can be described by universal equations. The dynamics of hydrogen and vapor pressure in manifolds can be described by ideal gas equation[18,19]:

$$\frac{dP_{h,\alpha}}{dt}=\frac{R_hT_\alpha}{V_\alpha}\left(\sum\dot{m}_{hin,\beta}-\sum\dot{m}_{hout,\beta}\right) \tag{1}$$

$$\frac{dP_{v,\alpha}}{dt}=\frac{R_vT_\alpha}{V_\alpha}\left(\sum\dot{m}_{vin,\beta}-\sum\dot{m}_{vout,\beta}\right) \tag{2}$$

Where α represents supply manifold (smf), inlet manifold ($inmf$) and outlet manifold ($outmf$). β represents proportional solenoid valve (pv), ejector ($ejct$), HRP (hrp), anode flow channel (an).

where $\dot{m}_{hin,\alpha}$ and $\dot{m}_{hout,\beta}$ are the hydrogen inlet mass flow rate and outlet mass flow rate of the manifold while $\dot{m}_{vin,\beta}$ $\dot{m}_{vout,\beta}$ are the water vapor inlet mass flow rate and outlet mass flow rate. $P_{h,\alpha}$ and $P_{v,\alpha}$ is the internal hydrogen and water vapor pressure, T_α is internal temperature, V_α is the volume of the manifold, R_h and R_v are the gas constant of hydrogen and water vapor.

The flow resistance from the manifold can be calculated according to the darcy-weisbach equation[20]:

$$P_{in,\beta}-P_\alpha=\lambda_\alpha\frac{l_\alpha}{d_\alpha}\frac{u_{in,\beta}^2}{2}\cdot\rho_{mix,\alpha} \tag{3}$$

$$P_\alpha-P_{out,\beta}=\lambda_\alpha\frac{l_\alpha}{d_\alpha}\frac{u_{out,\beta}^2}{2}\cdot\rho_{mix,\alpha} \tag{4}$$

$P_{in,\beta}$ and $P_{out,\beta}$ are the total inlet pressure and outlet pressure of the manifold, $u_{in,\beta}$ and $u_{out,\beta}$ are the total inlet and outlet flow velocity, l_α is the length of the manifold, A_α is the sectional area, d_α is the diameter of cross section, $\rho_{mix,\alpha}$ is the density of mixed gas in inlet or outlet of manifold, λ_α is the drag coefficient.

2.2 Anode flow channel

The filling dynamic of anode flow channel is similar to that of manifold. So the dynamics of the hydrogen and vapor pressure in anode and flow resistance can be modeled as same as manifold. However, the chemical reaction and water transport between the anode and the cathode cause the variation of components.

$$\dot{m}_{hreact,an}=M_h\frac{N_{st}I}{2F} \tag{5}$$

$$\dot{m}_{vtr,an}=\kappa M_v\frac{N_{st}I}{F} \tag{6}$$

where $\dot{m}_{hreact,an}$ is the hydrogen chemical reaction consumption, $\dot{m}_{vtr,an}$ is the water vapor mass flow rate transported across membranes, M_h and M_v are the molar mass of hydrogen and water vapor, F is the faraday constant, N_{st} is the number of stack cell, I is the load current of the stack, κ is the water diffusion coefficient.

When $P_{v,an}$ pressure of vapor in anode reaches the saturated vapor pressure, $P_{v,an}$ no longer increases and liquid water is formed, and liquid water mass can be calculated as:

$$m_{v,liquid}=\frac{V_{an}}{R_vT_{an}}\left(P_{v,an}-P_{sat}\right) \tag{7}$$

Where $m_{v,liquid}$ is the liquid water mass in anode, P_{sat} is the saturated vapor pressure under the temperature T_{an}.

2.3 Proportional solenoid valve

The flow characteristic of PV can be regarded as nozzle flow. Changing the opening of the PV will affect the pressure difference, making the flow state in subcritical or supercritical. Hydrogen mass flow rate can be described as:

$$\dot{m}_{h,pv}=\begin{cases}\dfrac{514\sqrt{P_{hout,pv}\Delta P}}{\sqrt{T_{h,pv}\rho_{h,pv}}}\cdot K_{v,pv} & P_{hout,pv}\geq\dfrac{P_{hin,pv}}{2}\\ \dfrac{257P_{hin,pv}}{\sqrt{T_{h,pv}\rho_{h,pv}}}\cdot K_{v,pv} & P_{hout,pv}<\dfrac{P_{hin,pv}}{2}\end{cases} \tag{8}$$

Where

$$\Delta P=P_{hin,pv}-P_{hout,pv} \tag{9}$$

Where $\dot{m}_{h,pv}$ is the output hydrogen mass flow rate of the PV, $P_{hin,pv}$ is the pressure of PV inlet, $P_{hout,pv}$ is the pressure of PV outlet, $K_{v,pv}$ is the flow coefficient, $T_{h,pv}$ is the temperature of hydrogen at PV inlet, $\rho_{h,pv}$ is the density of the hydrogen at PV inlet.

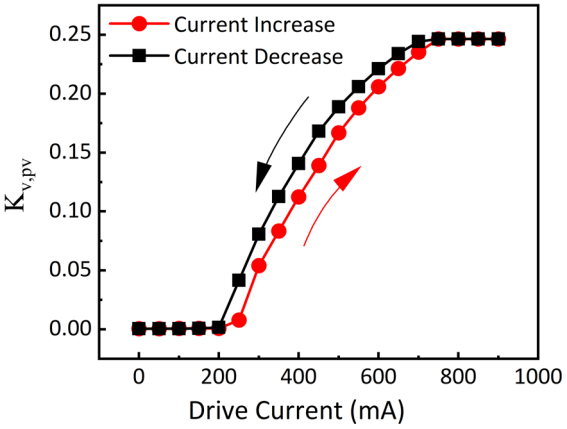

Fig.2 The flow performance of PV.

Fig.2 depicts the flow performance of the PV. PV can only be opened when the drive current is between 200mA to 750mA. Due to the influence of viscous friction and inertance, PV can not be closed to the specified position when drive current decreases. Therefore, flow coefficient in drive current increasing condition is less than in decreasing condition even the drive current is same.The modeling method of MPV and purge valve are as same as the PV so that it is not repeatedly described.

2.4 HRP

The outlet mass flow rate of the HRP depends on the inlet pressure, pressure difference and the motor speed.

$$\dot{m}_{out,hrp} = f\left(P_{in,hrp}, \Delta P_{hrp}, n_{hrp}\right) \tag{10}$$

Where

$$\Delta P_{hrp} = P_{out,hrp} - P_{in,hrp} \tag{11}$$

Where $\dot{m}_{out,hrp}$ is the outlet mass flow rate of the HRP, $P_{in,hrp}$ is the inlet pressure, ΔP_{hrp} is pressure difference, n_{hrp} is the motor speed.

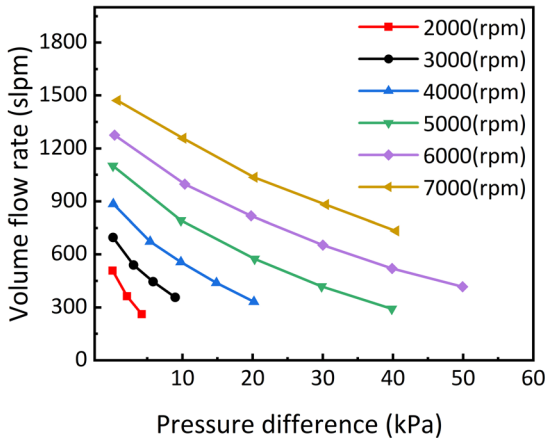

Fig.3 The flow rate performance MAP of the HRP.

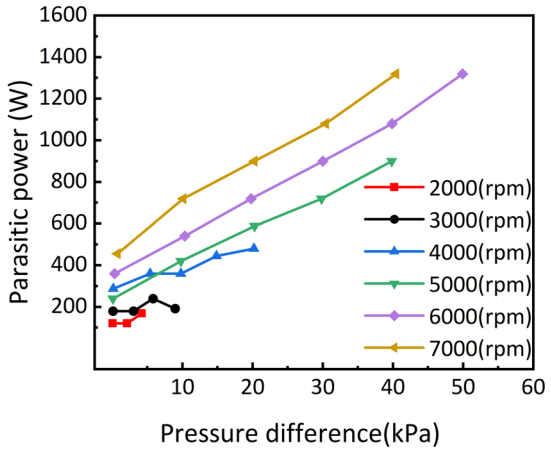

Fig.4 The parasitic power MAP of the HRP.

Fig.3 depicts the flow characteristics of the HRP under the 250kPa inlet pressure. As the pressure difference increases, the outlet flow rate decreases because more energy will be used to enhance the flow pressure. As the motor speed increases, the flow curve moves towards the upper right. Furthermore, with influence of inlet pressure HRP can recycle more hydrogen by increasing same motor speed under the high inlet pressure. Fig.4 depicts the parasitic power performance of the HRP under the 250kPa inlet pressure. As the pressure difference increases, the parasitic power of the HRP increases because it needs to apply more work to raise the pressure of the hydrogen.

2.5 Ejector

The modeling approach of ejector can be borrowed from blower. The flow rate of primary fluid can be equivalent to motor speed of blower which decides the circulation capacity. And pressure difference can be described as outlet and secondary inlet pressure of ejector. Recycle performance of ejector can be described as:

$$\dot{m}_{s,ejct} = f\left(\dot{m}_{p,ejct}, \Delta P_{ejct}\right) \tag{12}$$

Where

$$\Delta P_{ejct} = P_{out,ejct} - P_{s,ejct} \tag{13}$$

Where $\dot{m}_{s,ejct}$ and $\dot{m}_{p,ejct}$ are the secondary and primary fluid mass flow rate of ejector, $P_{s,ejct}$ and $P_{out,ejct}$ are the pressure of secondary fluid and outlet fluid.

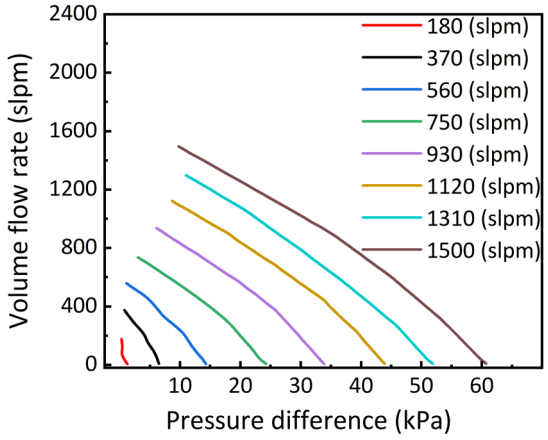

Fig.5 The recycle flow rate performance MAP of ejector in different primary flow rate.

Fig.5 depicts the recycle performance of ejector. As pressure difference increases, more energy is used to raise pressure of the fluid. When the pressure of secondary fluid is less than the low pressure area at the nozzle outlet, counterflow occurs. In addition, as primary flow rate increases which means that circulation capacity raises, the flow rate curve moves towards upper right.

2.6 Model validation

In this work, the experiment data is derived from a real 130kW fuel cell system. The PV, HRP and ejector are modeled with data-driven methods. The output characteristics of these components are calculated with interpolation method based on test data shown as Fig.2~Fig.5.

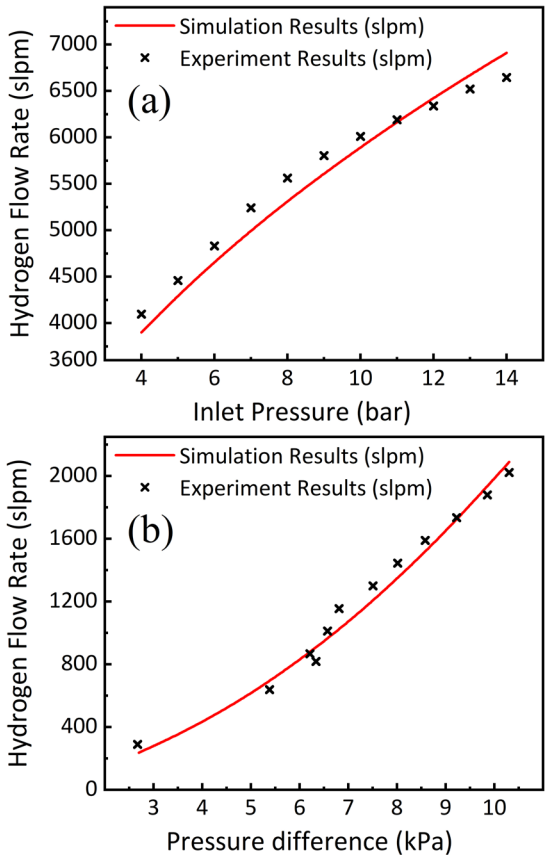

Fig.6 The results of model validation. (a) is the MPV model validation. (b) is the anode model validation.

The model accuracy of MPV are verified by comparing the experimental and simulated values of output flow rate under different inlet pressure shown as Fig.6(a) which the maximun error are 4.79%. Fig.6 (b) illustrates the hydrogen flow rate of anode inlet under step-change power condition. The flow rate of simulaiton can follow the experiment results and error is within reasonable limits. Therefore, the hydrogen supply system model established in this paper has high accuracy and can be used to further research on circulation structure analysis.

3. SINGLE EJECTOR CIRCULATION STRUCTURE

In different operating condition, the hydrogen requirement and flow resistance of fuel cell stack are also different. In order to improve the electrochemical reaction speed of fuel cell stack, the flow rate of hydrogen supplied to the fuel cell stack is usually greater than the actual demand for current reaction. According to Eq.(5), the hydrogen stoichiometric ratio (STR) is described as:

$$\lambda_h = \frac{\dot{m}_{hin,an}}{\dot{m}_{hreact,an}} \tag{14}$$

where $\dot{m}_{hreact,an}$ is hydrogen reaction consumption, $\dot{m}_{hin,an}$ is the hydrogen inlet mass flow rate of the anode.

According to the matching requirements of the selected stack and real experiment of 130kW fuel cell system, flow resistance and the required hydrogen flow rate under different output power are shown as Table.1. Single ejector scheme is shown as Fig.7.

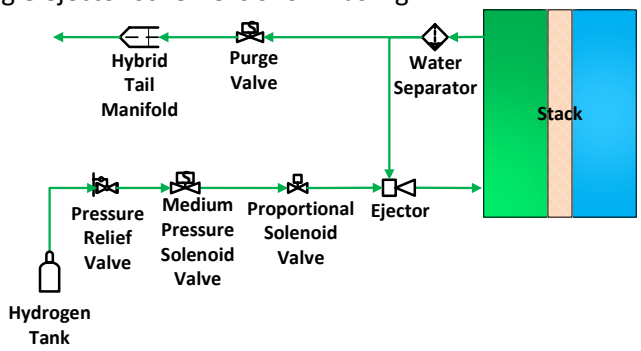

Fig.7 Hydrogen supply system in single ejector scheme.

Table. 1 Fuel cell stack hydrogen and pressure rise requirements

Current (A)	Output Power (kW)	STR (-)	Flow rate of recycle hydrogen (slpm)	Flow rate of fuel cell stack inlet hydrogen (slpm)	Flow rate of hydrogen consumption (slpm)	Fuel cell anode inlet pressure (kPa)	Flow resistance (kPa)
33	12	3	193	289	96	134	2.7
99	33	2.5	434	723	289	171	7.9
165	54	1.7	337	819	482	208	6.3
231	74	1.5	337	1012	675	239	6.6
297	93	1.5	434	1301	867	259	7.5
363	111	1.5	530	1590	1060	266	8.6
462	135	1.5	675	2024	1349	266	10.3

Because the hydrogen from hydrogen tank is dry hydrogen, the water vapor flow rate at the inlet of stack anode fully comes from the secondary inlet of ejector. Regarding the primary fluid hydrogen flow rate and the pressure difference between outlet and the secondary inlet of ejector as the input parameter of ejector model There is a simulation result for the single ejector recycle scheme shown as Fig.8.

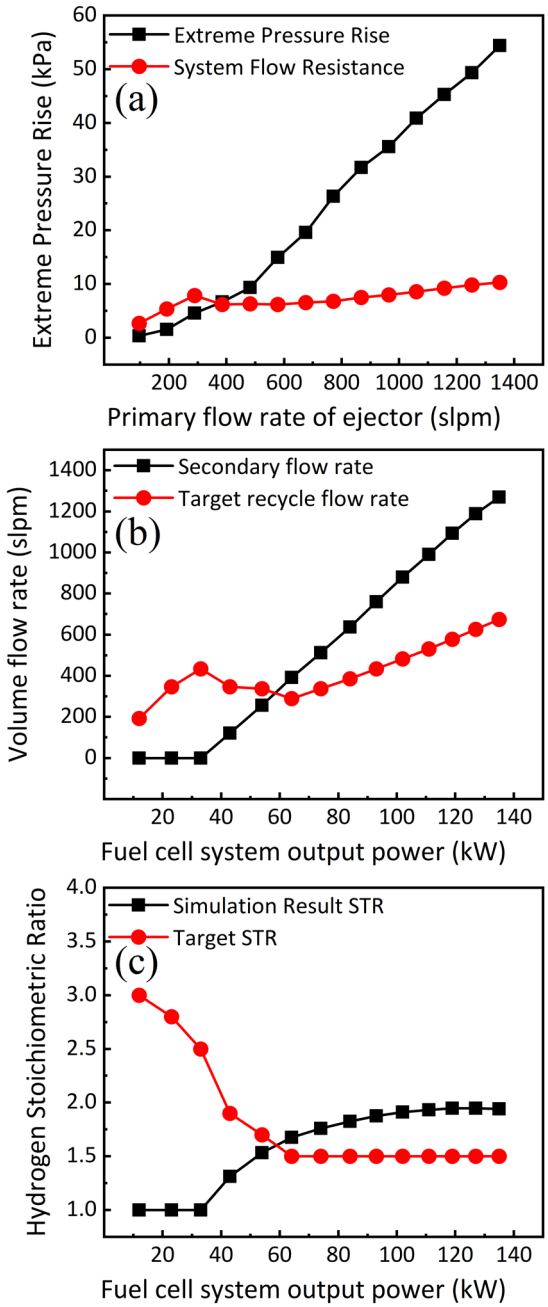

Fig.8 Single Ejector scheme simulation results. (a) is the comparation of system flow resistance and extreme pressure rise of ejector. (b) is the comparation of ejector secondary flow rate and target. (c) is the comparation of single ejector scheme STR and taget STR.

Fig.8 (a) is the comparation of system flow resistance and extreme pressure rise of ejector and Fig.8 (b) is the comparation of ejector secondary flow rate and target recycle flow rate. As the system power is loaded from 0 to 135kW, the primary flow rate of ejector rises from 0 to 1349slpm. The ejector extreme pressure rise is lower than the system flow risistance when the power is less than 33kW, which means the ejector can not recycle any hydrogen. As the power is between 43 to 60kW, ejector can overcome the system flow resistance and recycle some of the hydrogen but not enough. When the power reaches 60kW or more, ejector recycle capacity is enough to recycle the hydrogen more than the target.

Fig.8 (c) is the comparation of single ejector scheme STR and taget STR. When the power reaches 60kW or more, the PV is closed-loop controlled to raise pressure of stack anode inlet by increasing the primary flow rate of ejector. In this dynamic process, as the only fluid entering the circulation loop, primary flow rate of ejector is greater than the stack consumption and the remaining hydrogen of the electrochemical reaction is retained in the circulation loop. When the pressure of stack anode inlet reachs the target, primary flow rate of ejector is controlled to reduce to the same as the stack consumption flow rate, and the flow rate comes to balance and the remained flow rate in circulation loop is greater than target recycle flow rate. Finally the result shows that the STR is greater than target STR.

4. PARALLEL AND SERIAL CIRCULATION STRUCTURES

4.1 Ejector and HRP parallel scheme

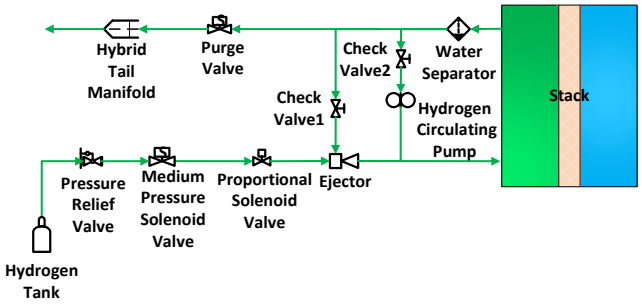

Fig.9 Hydrogen supply system structure with ejector and HRP parallel scheme.

Ejector and HRP parallel scheme divides the circulation loop into two lines which can avoid the influence of inefficient working area of ejector shown as Fig.9. With parallel scheme, the pressure difference between outlet and secondary inlet of ejector is as same as the pressure difference of HRP. Total recycle fluid mass flow rate is equal to the sum of secondary mass

flow rate of ejector and recycle fluid mass flow rate of HRP. Based on the recycle performance of ejector described by Fig.8, three working intervals are designed as single HRP working interval, HRP working with ejector interval and single ejector working interval. Two check valves are added to avoid counterflow shown as Fig.9.

When system output power is between 0 to 43kW, extreme pressure rise of ejector is lower than system fluid resistance and no unreacted hydrogen can be recycled by ejector. Therefore hydrogen supply system is designed to work in single HRP working interval. Check valve 1 is shut off to avoid counterflow and unreacted hydrogen is only recycled by HRP. Adjust the motor speed of HRP to make the HRP flow rate meet the requirement of target recycle flow rate.When system output power is between 43 to 60kW, ejector can overcome the system flow resistance but recycle insufficient hydrogen. Therefore, hydrogen supply system is designed to work in HRP working with ejector interval. Both of check valve 1 and check valve 2 are opened to keep two circulation lines. The remaining hydrogen can be recycled back by the HRP adjusting the motor speed. When system output power exceeds 60kW, ejector recycle capacity becomes powerful so that hydrogen supply system is designed to work in single ejector working interval. Check valve 2 is shut off and HRP keeps stop with 0 rpm motor speed.

4.2 Ejector and HRP serial scheme

Structure of Ejector and HRP serial scheme is shown as Fig.10. With serial scheme, hydrogen flow rate through HRP is as same as the flow rate through secondary inlet of ejector. Total pressure difference is equal to the sum of the pressure difference between outlet and secondary inlet of ejector and the pressure difference of HRP. Based on different recycle capacity of ejector in working range, two working internals are designed as HRP working with ejector interval and single ejector working interval.

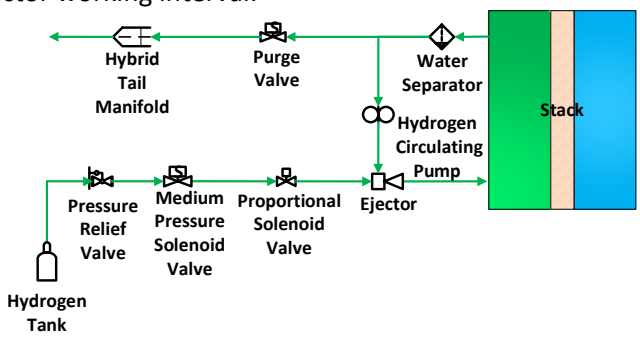

Fig.10 Hydrogen supply system structure with ejector and HRP serial scheme.

When system output power is between 0 to 60kW, hydrogen supply system is designed to work in HRP working with ejector interval. HRP undertakes the pressure rising work and help ejector establish pressure difference to accomplish ejection. When the flow rate through the manifold between ejector and HRP achieves balance, pressure difference by ejector and HRP are distributed completely. When system output power exceeds 60kW, hydrogen supply system is designed to work in single ejector working interval. In this interval, HRP is turned off and becomes a flow resistance source. Ejector has to overcome the system flow resistance but also provide addition power to help hydrogen overcome the resistance of the blades rotation from HRP. In simulaiton experiment, it is need to figure out when to turn off the HRP by decreasing the motor speed of HRP and keeping meet the requirement of recycle flow rate at the same time under different fuel cell system working operation.

4.3 Results Analysis

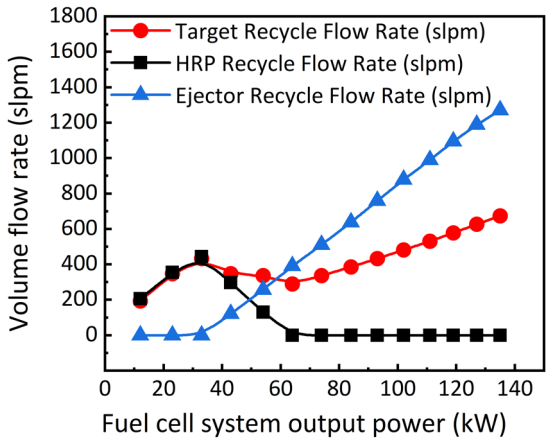

Fig.11 Recycle flow rate of components comparation in ejector and HRP parallel scheme.

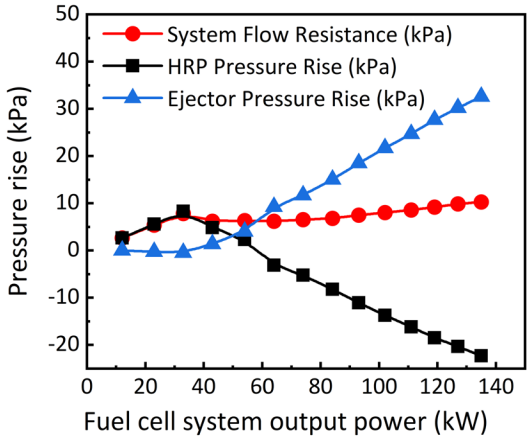

Fig.12 Pressure rise of components comparation in ejector and HRP serial scheme.

Fig.11 shows the recycle flow rate of components comparation in parallel scheme. When system output power is lower than 33kW, hydrogen supply system works in single HRP working interval and whole recycle flow rate is supplied by HRP. As the system output power increases from 33kW to 60kW, recycle capacity of ejector improves slowly and recycle flow rate by ejector increases. The motor speed of HRP is controlled to reduce the recycle flow rate by HRP. When the system output power exceeds 60kW, ejector can completely recycle all target circulation flow rate needed by fuel cell stack and HRP is shut off. Fig.12 is pressure rise of components comparation in ejector and HRP serial scheme. When system output power is lower than 33kW, counterflow occurs on the secondary inlet of ejector and ejector becomes a burden to HRP. HRP not only has to overcome the flow resistance from anode champer but also from the ejector. Pressure rise of HRP is a little greater than system flow resistance shown as Fig.12. The maximun flow resistance of ejector in working operation is 0.45kPa. When system output power is between 33 to 60kW, system flow resistance is shared by ejector and HRP. As the system output power increases, the primary flow rate of ejector increasing inproves the ejector capacity of overcoming flow resistance. Therefore, the motor speed of HRP can be reduced to minish the parasitic power. When system output power exceeds 60kW, HRP is shut off and become a burden to ejector. As the requirement of recycling hydrogen grows, flow resistance from HRP increases. The maximun flow resistance from HRP is 22.25kPa.

Fig.13 (a) and Fig.13 (c) are the recycle flow rate and STR comparation of single HRP scheme, Parallel scheme and serial scheme, respectively. Three circulation structure schemes can meet the requirement of recycle flow rate while overcoming system flow resistace. Single HRP scheme can control recycle flow rate accurately because HRP is a active component. When the system output power is lower than 33kW, recycle flow rate in all schemes is a little greater than target because the hydrogen recycle work is only undertaken by HRP with minimum motor speed 100 rpm. When system output power increases from 33kW to 60kW, in parallel scheme STR is greater than target. The reason is that ejector can recycle a part of flow rate but not enough and HRP has to keep minimum motor speed to help recycle hydrogen. In serial scheme the recycle flow rate through HRP is as same as ejector so that HRP controls recycle flow rate accurately with some flow resistance overcomed by ejector. As the system output power exceeds 60kW, STR in parallel scheme is greater than target with a maximun difference of 0.44 because ejector can make the best of capacity of recycling hydrogen due to cutted off HRP line. In serial scheme, part of hydrogen recycle capacity of ejector is used to overcome the flow resistance from HRP so that recycle flow rate is only a little greater than target with a maximun difference of 86.81 slpm.

Fig.13 (b) is parasitic power comparation of three scheme and Fig.13 (d) is parasitic power difference between parallel scheme and serial scheme when system power is lower than 60kW. Parasitic power difference is described as:

$$\delta_p = P_{series} - P_{parrallel} \tag{15}$$

Where δ_p is parasitic power difference between parallel scheme and serial scheme, and P_{series} is parasitic power in serial scheme and $P_{parrallel}$ is parasitic power in parallel scheme.

When system output power is lower than 33kW, parasitic power in single HRP shceme is as same as parallel scheme and serial scheme consumes the most parasitic power among three schemes. The reason is that in serial scheme HRP needs to establish high pressure of secondary inlet of the ejector to flow hydrogen through ejector in addition, shown as Fig.13 (d).

The parasitic power in serial scheme has a maximun 5.4W more than parallel scheme in 33kW system output power. This parasitic power difference depends on the mechanical structure dimension of the ejector. When system output power is between 33kW to 60kW, Parasitic power in parallel scheme has 16.9W lower than single HRP scheme under 54kW system output power while parasitic power in serial scheme has 54.5W lower than single HRP scheme. The reason is that the ejector participates in recycling hydrogen and motor speed of HRP can be decreased properly to save energy. In parallel scheme parasitic power is reduced by decreasing motor speed of HRP while parasitic power is reduced by decreasing pressure difference of HRP in serial scheme. Parasitic power in serial scheme has 37.6W lower than parallel scheme under 54kW indicating that influence on parasitic power reducing of decreasing the motor speed of HRP is more than decreasing the pressure difference. As system output power exceeds 60kW, parallel scheme and serial scheme consume no parasitic power because HRP is shut off. An average of parasitic power in parallel scheme can be reduced 190W than single HRP scheme under the premise of ensuring target recycle flow rate and overcoming system flow resistance while parasitic power in serial scheme can be reduced 200.8W.

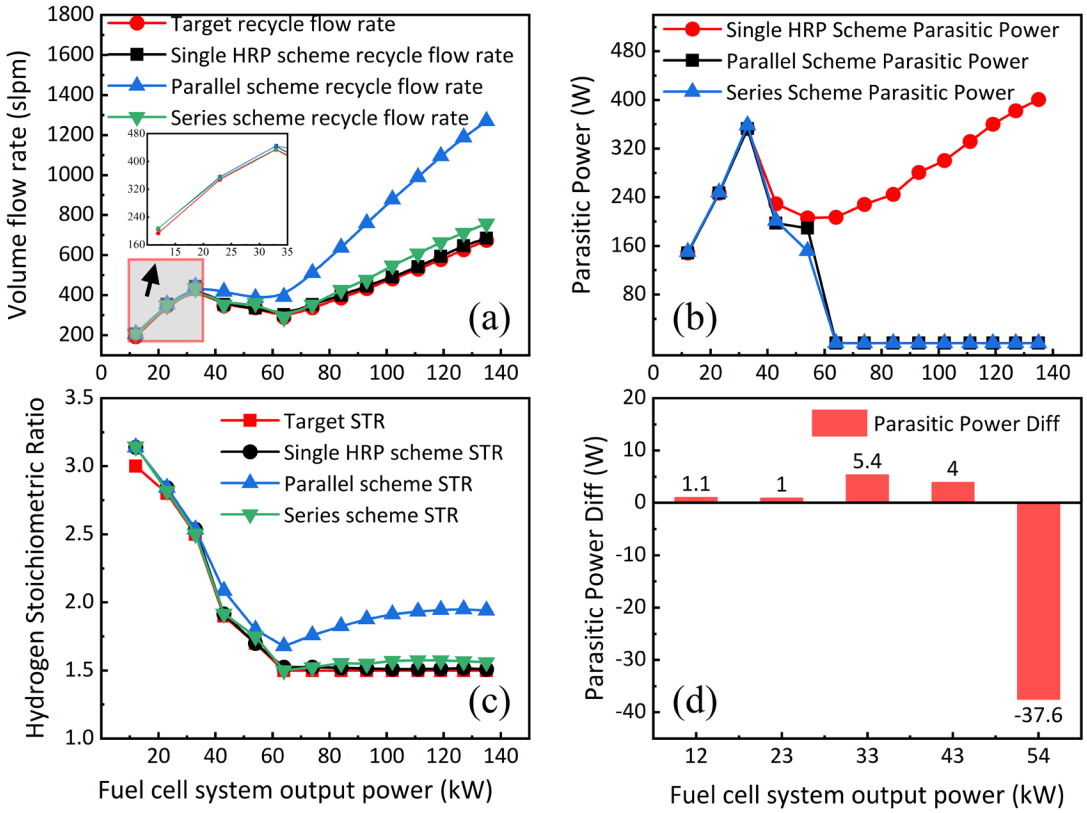

Fig.13 Three circulation structures simulation results. (a) is recycle flow rate comparation of single HRP scheme, Parallel scheme and serial scheme. (b) is parasitic power comparation of three schemes. (c) is STR comparation of three schemes. (d) is the parasitic power diff comparation of parallel scheme and serial scheme.

5. CONCLUSION

In this study, an accurate hydrogen supply system of fuel cell system model was established to research different circulation structures working characteristics.

Single ejector scheme and single HRP scheme were proposed to meet the requirement of unreacted hydrogen circulation and overcoming system flow resistance. The simulation results show that (1) in single ejector scheme counterflow occurs in system output power less than 33kW. As system output power increases, primary flow rate increasing helps improve circulation capacity of ejector and recycle hydrogen more than target. (2) In single HRP scheme hydrogen recycle flow rate is controlled accurately by HRP but high parasitic power is generated.

Ejector and HRP parallel scheme and serial scheme were proposed to solve the problem of high parasitic power of single HRP scheme and counterflow of single ejector scheme. In parallel scheme matching control strategy design consists of three working intervals and solves the counterflow by cutting off ejector line and recycling hydrogen only through HRP in system output power less than 33kW. An average of parasitic power in parallel scheme can be totally reduced 190W than single HRP scheme in whole fuel cell stack working operation and greater STR can be achieved. In serial scheme matching strategy controls HRP establish high pressure difference to solve counterflow and an average of parasitic power is totally reduced 200.8W than single HRP scheme.

However, further research (stack anode inlet pressure and flow rate control strategy and structure reliability etc.) is needed because the influence of the proposed structure scheme on flow characteristic is relatively complex. Based on the accuracy verification and the model of the proposed structure scheme in this paper, the fuel cell system efficiency can be further improved by mechanical structure dimension optimization design of ejector and selection of HRP.

ACKNOWLEDGEMENT

This work is supported in part by National Key R&D Plan of China (Grant No. 2023YFB4301604-08).

REFERENCE

[1] Sharma S, Ghoshal S K. Hydrogen the future transportation fuel: From production to applications[J].

Renewable and Sustainable Energy Reviews, 2015, 43: 1151-1158.
[2] Tai X Y, Zhakeyev A, Wang H, et al. Accelerating Fuel Cell Development with Additive Manufacturing Technologies: State of the Art, Opportunities and Challenges[J]. Fuel Cells, 2019, 19(6): 636-650.
[3] Nan Zequn, Xu Sichuan, Zhang Daobiao, et al. Development and prospect of hydrogen supply system in vehicle PEMFC[J]. Chinese Journal of Power Sources, 2016, 40(8): 1726-1730.
[4] Hwang J J. Effect of hydrogen delivery schemes on fuel cell efficiency[J]. Journal of Power Sources, 2013, 239: 54-63.
[5] Chen J, Siegel J B, Stefanopoulou A G, et al. Optimization of purge cycle for dead-ended anode fuel cell operation[J]. International Journal of Hydrogen Energy, 2013, 38(12): 5092-5105.
[6] Esbo M R, Ranjbar A A, Rahgoshay S M. Analysis of water management in PEM fuel cell stack at dead-end mode using direct visualization[J]. Renewable Energy, 2020, 162: 212-221.
[7] Badami M, Mura M. Theoretical model with experimental validation of a regenerative blower for hydrogen recirculation in a PEM fuel cell system[J]. Energy Conversion and Management, 2010, 51(3): 553-560.
[8] He H, Quan S, Wang Y X. Hydrogen circulation system model predictive control for polymer electrolyte membrane fuel cell-based electric vehicle application[J]. International Journal of Hydrogen Energy, 2020, 45(39): 20382-20390.
[9] Zhou R, Dong L, Liu H, et al. Excitation characteristics of lobe hydrogen circulating pump in polymer electrolyte membrane fuel cell under different clearances and pressure ratios[J]. Applied Thermal Engineering, 2023, 226: 120230.
[10] Kim M, Sohn Y J, Cho C W, et al. Customized design for the ejector to recirculate a humidified hydrogen fuel in a submarine PEMFC[J]. Journal of Power Sources, 2008, 176(2): 529-533.
[11] Wang X, Xu S, Xing C. Numerical and experimental investigation on an ejector designed for an 80 kW polymer electrolyte membrane fuel cell stack[J]. Journal of Power Sources, 2019, 415: 25-32.
[12] Hwang J J. Passive hydrogen recovery schemes using a vacuum ejector in a proton exchange membrane fuel cell system[J]. Journal of Power Sources, 2014, 247: 256-263.
[13] Ahluwalia R K, Wang Xiaohua. Fuel cell systems for transportation: Status and trends[J]. Journal of Power Sources, 2008, 177(1): 167-176.
[14] He J, Choe S Y, Hong C O. Analysis and control of a hybrid fuel delivery system for a polymer electrolyte membrane fuel cell[J]. Journal of Power Sources, 2008, 185(2): 973-984.
[15] Zhang Renjie, Jiang Peixue, Zhu Yinhai. Experimental Research on Ejection and Booster Scheme of Fuel Cell Anode Gas Recirculation System[J]. Journal of Engineering Thermophysics, 2023, 44(9): 2362-2368.
[16] Subramanian G, Natarajan S K, Adhimoulame K, et al. Comparison of numerical and experimental investigations of jet ejector with blower[J]. International Journal of Thermal Sciences, 2014, 84: 134-142.
[17] Dong L, Zhou R, Liu H, et al. Effect of rotational speed on unstable characteristics of lobe hydrogen circulating pump in fuel cell system[J]. International Journal of Hydrogen Energy, 2022, 47(50): 21435-21449.
[18] El-Sharkh M Y, Rahman A, Alam M S, et al. A dynamic model for a stand-alone PEM fuel cell power plant for residential applications[J]. Journal of Power Sources, 2004, 138(1-2): 199-204.
[19] Pukrushpan J T, Peng H, Stefanopoulou A G. Simulation and Analysis of Transient Fuel Cell System Performance Based on a Dynamic Reactant Flow Model[C]//Dynamic Systems and Control. New Orleans, Louisiana, USA: ASMEDC, 2002: 637-648.
[20] Haktanır T, Ardıçlıoğlu M. Numerical modeling of Darcy–Weisbach friction factor and branching pipes problem[J]. Advances in Engineering Software, 2004, 35(12): 773-779.